

Pattern formation, outbreaks, and synchronization in food chains with two and three species

Sabrina B. L. Araújo and M. A. M. de Aguiar

Instituto de Física “Gleb Wataghin,” Universidade Estadual de Campinas, Caixa Postal 6165, 13083-970 Campinas, São Paulo, Brazil

(Received 28 November 2006; revised manuscript received 1 February 2007; published 14 June 2007)

We study the dynamics of populations of predators and preys using a mean field approach and a spatial model. The mean field description assumes that the individuals are homogeneously mixed and interact with one another with equal probability, so that space can be ignored. In the spatial model, on the other hand, predators can prey only in a certain neighborhood of their spatial location. We show that the size of these predation neighborhoods has dramatic effects on the dynamics and on the organization of the species in space. In the case of a three species food chain, in particular, the populations of predators display a sequence of apparently irregular outbreaks when the predation neighborhood has intermediate values, as compared to the size of the available space. Nonetheless, further increasing their size makes the outbreaks disappear and the dynamics approach that of the mean field model. Our study of synchronization also shows that the periodic behavior displayed by the average populations in a spatially extended system may hide the existence of patches that oscillate out of phase in a highly coordinated fashion.

DOI: [10.1103/PhysRevE.75.061908](https://doi.org/10.1103/PhysRevE.75.061908)

PACS number(s): 87.23.Cc, 87.18.Hf, 87.17.Aa

I. INTRODUCTION

The use of mathematical models to describe the time evolution of ecological systems dates back to Lotka [1] and Volterra [2]. Since their pioneering work several different models have been proposed to describe a variety of interactions, from predation and parasitism to mutualism. The time evolution of interacting populations can be modeled in several ways, including differential equations, discrete time maps, and spatial models. Which of these are more appropriate depends on the problem at hand and on the degree of detail one wishes to describe. At the lowest level of detail, where only the total number of individuals of each species is important, the dynamics can be most simply described by mean field models, where space is ignored. However, the large amount of new observational data on the spatial distribution of several species that has become available in the last years has driven new empirical and theoretical studies of spatial models [3,4].

The main appeal of spatial models is the possibility of understanding not only the variation of the number of individuals of each species as a function of the time but also their spatial organization, the possibility of synchronization of patches of local populations, and the dynamics of outbreaks [5–12]. Synchronization is a particularly important subject that has attracted a lot of attention [13] and has been observed in measles [14], voles [15], lynxes [16,17], and microbes [18], among other biological systems. The phenomenon of synchronized outbreaks, that apparently cannot be described by mean field methods, has been observed in several species of insects, like moths, butterflies, cicada, and beetles [19–24]. It has been suggested [20] that environmental inhomogeneities in space or their changes over time, like cool springs, can synchronize the outbreak peaks in different places around the world. However, the synchronization tends to decrease with the distance between local populations [21–23] suggesting that local spatial interactions may also play an important role in the process. The migration of individuals may be one such interaction [17,21]. Synchronization

of coupled systems have been observed in other contexts, as well. The synchronization of chaotic dynamics has been intensively studied in a variety of systems since the 1990s [25–34].

In ecology, a particularly important mean field model was proposed by Hastings and Powell [35] to describe the dynamics of a three species food chain. In this model the population of each species is represented by a continuous variable satisfying a set of differential equations that incorporate pairwise nonlinear interactions with a Holling type-II functional response [36] (see next section for the details). As a mean field model, it assumes homogeneously mixed populations and space is not taken into account. Depending of the values of the model parameters, chaotic behavior, and strange attractors might emerge. Although very interesting, chaotic behavior does not seem to be common in natural populations [37–39]. Among the factors that might stabilize the chaotic dynamics is the nonhomogeneity of the spatial distribution of the populations [40].

In this paper we take the model of Hastings and Powell (hereafter called HP) as a basis to construct a spatial version of the three species food chain. We study the transition between regimes of different behaviors, particularly between behaviors where the spatial description is important, and behaviors that can be described by long range interactions assumed by the mean field approach. By studying this transition, we are able to understand which dynamical features are characteristic of the specific approach of the model, mean field or spatial, and which are robust and depend only on the types of interactions included in the equations. We shall see that not only is chaos largely minimized by local interactions, but also that these interactions promote spatial organizations and may lead to outbreaks of predators. Long range interactions, on the other hand, tend to synchronize the population oscillations, leading to smoother spatial patterns and to overall chaotic behavior.

In order to include space and still have a computationally tractable dynamics, we have opted to work with discrete time. However, the construction of discrete time models preserving all properties of the corresponding set of differential

equations is strictly possible only if the equations are integrable. Since the HP model is nonintegrable, we have modified the equations slightly. In particular, we replaced the Holling response functions by different types of pairwise coupling and studied the dynamical behavior of the populations for four types of such functions. The guiding principle in building the discrete time equations was to preserve the qualitative features of the HP model. Space was introduced as a lattice of $N \times N$ sites, either with periodic boundary conditions, to simulate large environments, or with “hard walls” at the boundaries, to represent confined environments.

With the objective of understanding the dynamics with discrete time and the inclusion of space, we have first considered the interaction of only two species, a prey and a predator. Later we added a second predator that preys on the first predator. In both cases, the key ingredients of the spatial model are the possibility of migration to nearby sites and the constraint that predators can only prey in a certain neighborhood of their spatial location. We shall see that the size of these neighborhoods plays a crucial role in the dynamics and in the spatial organization of the species. When the predation neighborhood has intermediate values, small compared to the size of the available space, but large compared to a single patch of the model, outbreaks of predators may arise. We call the local bursts of predators “superpopulations.” Increasing the size of the predation neighborhoods beyond the intermediate values makes the superpopulations of predators disappear and causes the dynamics to approach that of the mean field model.

This paper is organized as follows: in Sec. II we briefly review the HP model. In Sec. III we construct discrete time versions of the HP model and generalize them to include space. In Secs. IV and V we present our results for the cases of two and three species, respectively, and in Sec. VI we summarize our conclusions.

II. MODEL OF HASTINGS AND POWELL

Hastings and Powell [35] proposed a model to describe a three species food chain in which the species at the lowest level of the food chain, X , is preyed by the intermediate species Y , which, in turn is preyed by Z . The model is a canonical representation of pairwise interactions between the three species which incorporates a Holling type-II functional response [36] in both consumer species, namely Y and Z . The differential equations governing the evolution of the densities of each population are given by

$$\begin{aligned} \frac{dX}{dT} &= R_0 X \left(1 - \frac{X}{K_0} \right) - C_1 F_1(X) Y, \\ \frac{dY}{dT} &= F_1(X) Y - F_2(Y) Z - D_1 Y, \\ \frac{dZ}{dT} &= C_2 F_2(Y) Z - D_2 Z, \end{aligned} \quad (1)$$

where

$$F_i(U) = \frac{A_i U}{B_i + U}, \quad i = 1, 2. \quad (2)$$

is the Holling type-II function [36]. At low prey densities U predation is an increasing function of U , whereas as prey density increases the rate of predator consumption levels off because each predator is able to handle only a finite number of prey per unit of time.

It is assumed that X is the only species that can survive on its own, R_0 being its intrinsic growth rate. However, X cannot grow indefinitely, and its population is limited by the carrying capacity K_0 . The Y type, on the other hand, needs X to survive. Its growth rate due to X is represented by $F_1(X)$. This function has a maximum value A_1 that restricts the growth of Y predators. The role of $F_2(Y)$ is similar to that of $F_1(X)$ and refers to the predation of Z upon Y . The parameters $1/C_1$ and C_2 are conversions rates of preys, X and Y , into predators Y and Z , respectively. Finally, the species Y and Z have intrinsic death rates, D_1 and D_2 , respectively.

III. MEAN FIELD AND SPATIAL MODELS WITH DISCRETE TIME

A. Mean field with discrete time

One of the difficulties in extending the HP model to a spatial formulation is that it would involve three coupled nonlinear partial differential equations, which can be very difficult to handle numerically. To avoid dealing with such equations we first propose a discrete time model based on the HP model. In order to do that, we first consider the behavior of each species in isolation, given by

$$\frac{dX}{dT} = R_0 X \left(1 - \frac{X}{K_0} \right), \quad \frac{dY}{dT} = -D_1 Y, \quad \frac{dZ}{dT} = -D_2 Z. \quad (3)$$

To reduce the number of parameters, Eqs. (3) can be scaled according the transformations [35] $x = X/K_0$, $y = Y/K_0$, $z = Z/K_0$, $t = TR_0$, $d_1 = D_1/R_0$, and $d_2 = D_2/R_0$. We obtain

$$\frac{dx}{dt} = x(1-x), \quad \frac{dy}{dt} = -d_1 y, \quad \frac{dz}{dt} = -d_2 z. \quad (4)$$

These equations can be readily integrated and a direct map between x , y , and z at time t and at time $t + \tau$ is obtained. Since the time t is measured in units of the inverse growth rate of the X type, we can take $\tau = 1$ and measure time steps in the same units. We obtain

$$\begin{aligned} x(t+1) &= \frac{x(t)}{x(t)(1-e^{-1}) + e^{-1}}, & y(t+1) &= y(t)e^{-d_1}, \\ z(t+1) &= z(t)e^{-d_2}. \end{aligned} \quad (5)$$

The dynamics generated by this map is identical to that of Eqs. (4), only calculated at discrete values of time. However, the interaction terms cannot be simply included and integrated in the same fashion, since the full HP model is non-integrable. Therefore the pairwise interactions must be added directly into the map, changing the details of the dynamics with respect to the original model. The idea is to preserve as much as possible the general properties of the system. We include the interactions as follows:

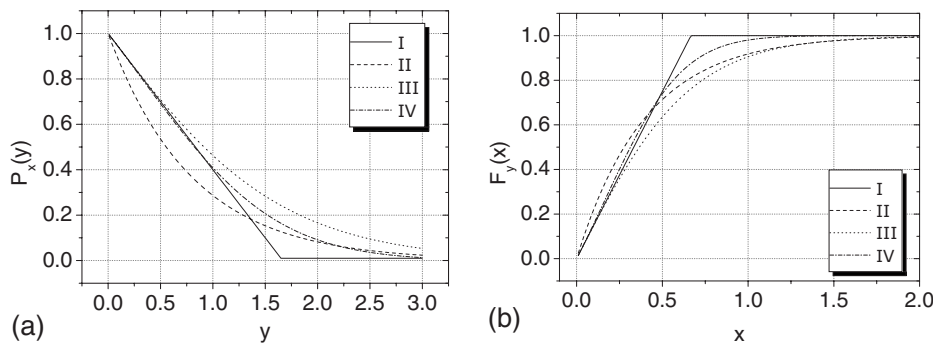


FIG. 1. Four types of response functions: (I) linear; (II) exponential; (III) hyperbolic tangent with linear argument; (IV) hyperbolic tangent with quadratic argument. (a) Predation function of y upon x , and (b) feeding function of y upon x .

$$\begin{aligned}
 x_{n+1} &= \left(\frac{x_n}{x_n(1 - e^{-1}) + e^{-1}} \right) P_x(y_n), \\
 y_{n+1} &= y_n [e^{-d_1} + F_y(x_n)] P_y(z_n), \\
 z_{n+1} &= z_n [e^{-d_2} + F_z(y_n)], \tag{6}
 \end{aligned}$$

where $P_h(g)$ accounts for the predation of g upon the prey h and $F_g(h)$ for the reproduction of g due to the feeding upon h . Therefore F adds to the growth rate, whereas P imposes an overall decrease of the population due to predation.

There are several possible choices for both P and F [41], as there are several choices for the pairwise interaction functions of continuous time models [36]. Each choice changes the details of the dynamics and corresponds to slightly different models. Below we list the four possibilities we have investigated, which are also displayed in Fig. 1. The first set corresponds to the simplest possible choice, namely, to functions that are linear by parts. These, however, have a discontinuity in the first derivative that can affect the dynamics. This effect can be studied by comparing the dynamics with that generated by the functions in the other three sets, which are smooth approximations to those in the first set.

Set I—linear:

$$\begin{aligned}
 P_h(g) &= \begin{cases} 1, 0 - 0,6g & \text{if } g < 1,65 \\ 0,01 & \text{if } g \geq 1,65 \end{cases}, \\
 F_y(x) &= \begin{cases} 1,5x & \text{if } x \leq 0,667 \\ 1,0 & \text{if } x > 0,667 \end{cases}, \\
 F_z(y) &= \begin{cases} 2,0y & \text{if } z \leq 0,5 \\ 1,0 & \text{if } z > 0,5 \end{cases}. \tag{7}
 \end{aligned}$$

We set the minimum value $P_h(g)$ at slightly above zero to avoid extinction of the three species. Here, and also in the three other cases below, we use the same function $P_h(g)$ for $P_x(y)$ and $P_y(z)$.

Set II—exponential:

$$\begin{aligned}
 P_h(g) &= e^{-g/0,8}, \\
 F_y(x) &= 1,0 - e^{-x/0,4}, \\
 F_z(y) &= 1,0 - e^{-y/0,2}. \tag{8}
 \end{aligned}$$

Set III—hyperbolic tangent with linear argument:

$$\begin{aligned}
 P_h(g) &= 1,0 - \tanh(0,6g), \\
 F_y(x) &= \tanh(1,5x), \\
 F_z(y) &= \tanh(2,6y). \tag{9}
 \end{aligned}$$

Set IV—tangent hyperbolic with quadratic argument:

$$\begin{aligned}
 P_h(g) &= 1,0 - \tanh(0,6g + 0,08g^2), \\
 F_y(x) &= \tanh(1,5x + 0,8x^2), \\
 F_z(y) &= \tanh(2,6y + 2,0y^2). \tag{10}
 \end{aligned}$$

The numerical coefficients appearing in the functions P and F were chosen to reproduce the typical behavior assumed by the variables x , y , and z in the HP model: a cycle when z is absent and a chaotic attractor when z is considered. These coefficients will be held fixed through out this paper.

B. Discrete spatial model

We introduce space as a two dimensional lattice with $N \times N$ sites, or patches. Each patch contains a small ecosystem with individuals of the three species. We assume that the predators in a given patch can feed only from preys that are sufficiently close to its home location. Each type of predator (y or z) is assigned a predation radius (R_y or R_z) such that preys inside a circle with that radius are equally likely to be predated, whereas preys outside that range are not attacked. This circular area around each predator is called its “predation neighborhood” [42]. A study of the robustness of pattern formation under these sharply defined neighborhoods can be found in [43]. We also assume that the individuals can migrate to the four nearest patches with rates m_x , m_y , and m_z for species X , Y , and Z , respectively.

The variables x , y , and z of the mean field model can be thought to represent the average density of the spatially distributed populations, with the feeding and predation functions evaluated at these global average values. In the spatial model with restricted predation ranges, it is reasonable to replace the feeding function $F_g(h)$ by an interaction that retains the same functional form but that depends on the average number of preys taken only on the predation neighborhood of each patch (i, j) :

$$F_g(h) \rightarrow F_g(\langle h \rangle_{R_g^{i,j}}) = F_g\left(\frac{1}{N_{R_g}} \sum_{l,m=-R_g}^{R_g} h^{i+l,j+m}\right). \quad (11)$$

The sum is restricted to the circular neighborhood of radius R_g , i.e., $\sqrt{l^2+m^2} \leq R_g$, and N_{R_g} is the number of patches in this neighborhood, which is roughly πR_g^2 . In the limit where R_g becomes of the order of the total available space the average recovers its mean field value.

The predation function also has to change to take into account the predation neighborhoods. To understand how this works we notice that the predators in the patch $(i+l, j+m)$ are able to predate in the patch (i, j) only if $\sqrt{l^2+m^2} \leq R_g$. Since there are N_{R_g} patches that can reach into (i, j) , each one contributes, on the average, $1/N_{R_g}$ to the total predation function at (i, j) . The contribution of the predators of the patch $(i+l, j+m)$ is

$$P_h^{i,j}(g^{i+l,j+m}) = \frac{1}{N_{R_g}} P_h(g^{i+l,j+m}). \quad (12)$$

Summing over all these patches we obtain the new predation function

$$\langle P_h^{i,j}(g) \rangle_{R_g} = \frac{1}{N_{R_g}} \sum_{l,m=-R_g}^{R_g} P_h(g^{i+l,j+m}), \quad \text{where } \sqrt{l^2+m^2} \leq R_g. \quad (13)$$

Figure 2 shows an illustration of the spatial lattice and the predation neighborhoods. With these considerations, our discrete spatial model assumes the form

$$x_{n+1}^{i,j} = \left(\frac{x_n^{i,j}}{x_n^{i,j}(1-e^{-1}) + e^{-1}} \right) \langle P_x(y_n) \rangle_{R_y(i,j)} + \frac{m_x}{4} \left(\sum_{l,m} 'x^{i+l,j+m} \right) - m_x x^{i,j},$$

$$y_{n+1}^{i,j} = y_n^{i,j} [e^{-d_1} + F_y(\langle x_n \rangle_{R_x(i,j)})] \langle P_y(z_n) \rangle_{R_z(i,j)} + \frac{m_y}{4} \left(\sum_{l,m} 'y^{i+l,j+m} \right) - m_y y^{i,j},$$

$$z_{n+1}^{i,j} = z_n^{i,j} [e^{-d_2} + F_z(\langle y_n \rangle_{R_y(i,j)})] + \frac{m_z}{4} \left(\sum_{l,m} 'z^{i+l,j+m} \right) - m_z z^{i,j}. \quad (14)$$

The prime in the sum over l and m indicates that the sum is restricted only to the four nearest neighbors of the site (i, j) .

To simulate the dynamics of two species we only need to make $z=0$ in Eqs. (6) and (14). In this case, the mean field equations become simply

$$x_{n+1} = \left(\frac{x_n}{x_n(1-e^{-1}) + e^{-1}} \right) P_x(y_n),$$

$$y_{n+1} = y_n [e^{-d_1} + A_y(x_n)], \quad (15)$$

and its spatial version

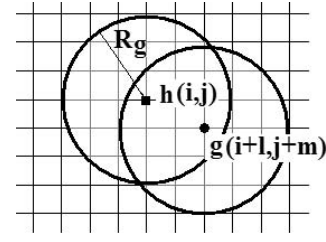


FIG. 2. Illustration of the spatial lattice and the predation neighborhoods.

$$x_{n+1}^{i,j} = \left(\frac{x_n^{i,j}}{x_n^{i,j}(1-e^{-1}) + e^{-1}} \right) \langle P_x(y_n) \rangle_{R_y(i,j)} + \frac{m_x}{4} \left(\sum_{l,m} 'x^{i+l,j+m} \right) - m_x x^{i,j}, \quad (16)$$

$$y_{n+1}^{i,j} = y_n^{i,j} [e^{-d_1} + F_y(\langle x_n \rangle_{R_x(i,j)})] + \frac{m_y}{4} \left(\sum_{l,m} 'y^{i+l,j+m} \right) - m_y y^{i,j}.$$

As a final remark, we emphasize that the present model is *not* an individual based cellular automaton, where each site contains at most one individual. Here, each site (that we also call a *patch*), contains a small ecosystem, with individuals of the three species. For reviews of the different types of spatial models commonly used in ecology, including the individual based model, patch models, and reaction diffusion systems, see [44,45]. In the next two sections we present several numerical results for the dynamics of two and three species both for the mean field and the spatial model. We focus on the comparison between the two approaches and on relevance of space in such dynamical systems.

IV. TWO SPECIES

We start the discussion of our results with the case of two species. This problem contains all the important elements

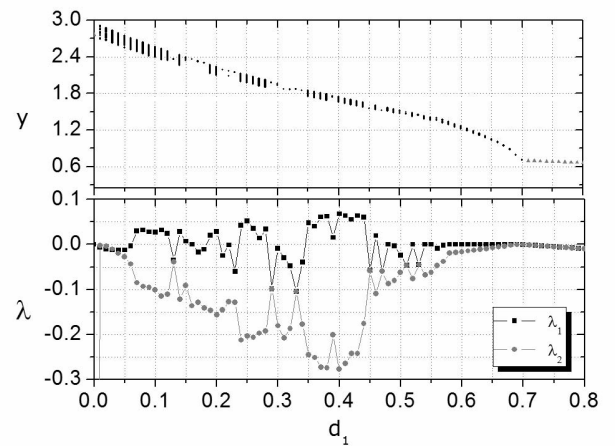


FIG. 3. Top: bifurcation diagram for the two species mean field model with linear predation and feeding functions. The circles (black) correspond to the maximum values of y in each oscillation plotted against d_1 , the death rate of species y . The triangles (gray) represent regimes where the dynamics converged to a fixed point. Bottom: Lyapunov exponents as a function of d_1 .

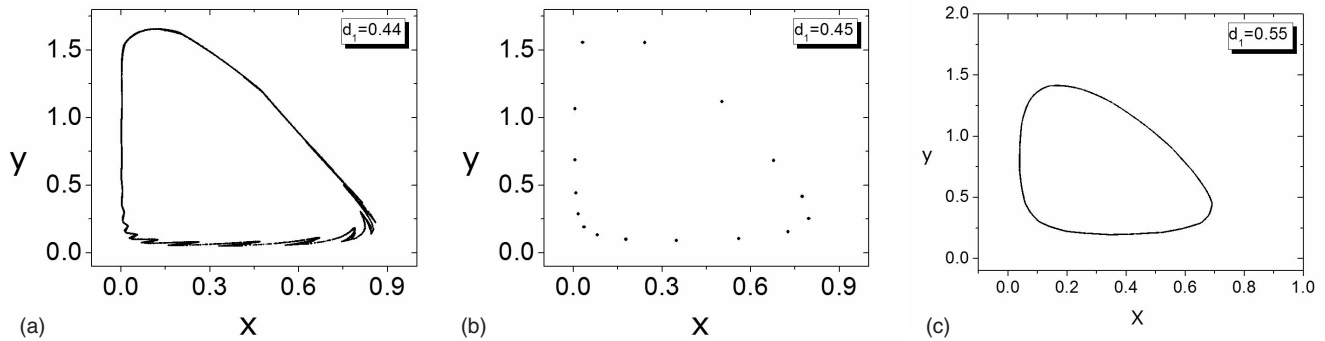


FIG. 4. Attractors for set I of functional responses for three different values of d_1 , indicated in the panels: (a) chaotic attractor; (b) periodic orbit; (c) limit cycle.

involved in the transition between the mean field and the spatial model and is simpler than that of three species. We shall see, however, that the introduction of the third species has very important consequences. Because of the large number of parameters of the model we have fixed the migration rates at $m_x=0.01$ and $m_y=0.1$ throughout the paper. In the present case of two species, the only free parameter in the mean field approach becomes d_1 , the death rate of the predator. When space is introduced, we shall also vary R_y , the size of predation neighborhood for the species y . In all cases the spatial lattice will be a square with $64 \times 64=4096$ sites. A discussion about the effects of different system sizes is left to Sec. VI.

A. Mean field model for two species

We performed a preliminary analysis of the dynamical behavior of x and y for each of the four types of predation

and feeding functions introduced in Sec. III using bifurcation diagrams and Lyapunov exponents [46]. It turns out that the most interesting and rich case is obtained with the linear functions. Figure 3 shows the bifurcation diagram and the Lyapunov exponents for this case as a function of d_1 . The bifurcation diagram is constructed as follows: Eqs. (15) are iterated for a large number of steps (14 000 in this case) and, after an initial transient is discarded (the first 4000 steps), both the x and y variables set into an oscillatory behavior. We take the maximum value attained by y in each of its oscillations and plot the whole set of maximum values as a function of d_1 . If the motion is periodic, the set consists of a finite number of points. If the motion covers a limit cycle or a chaotic region, the set will span a small interval. For $d_1 > 0.7$ the orbits converge to fixed points, which are also shown in the bifurcation diagram. To calculate the Lyapunov exponents we performed 200 000 iterations, also discarding

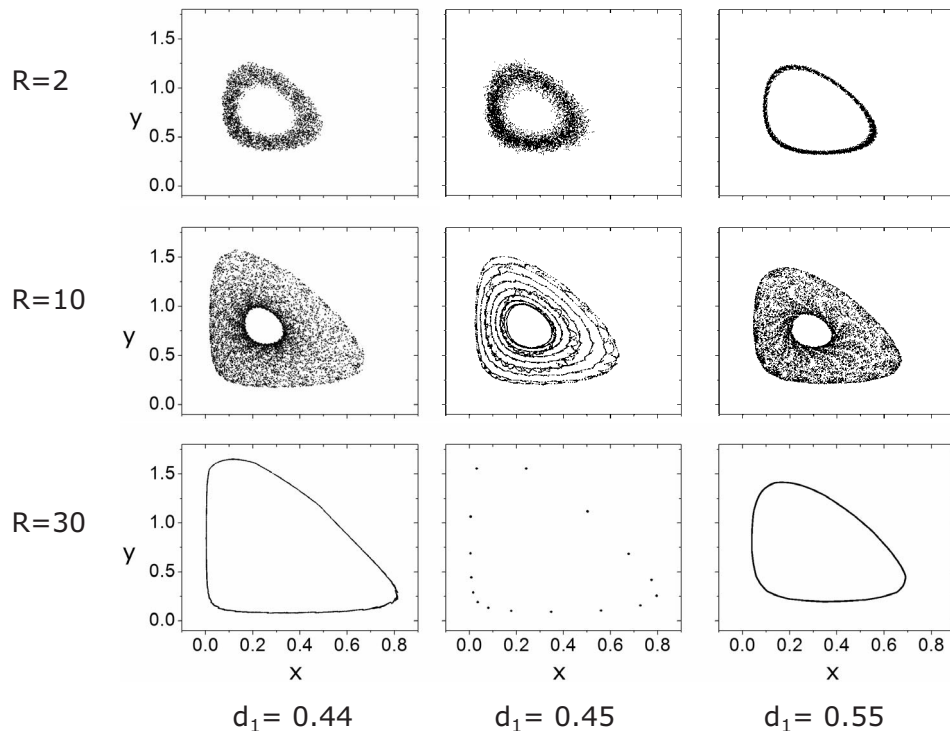


FIG. 5. Attractors for different values of d_1 and predation radius R considering periodic boundary conditions. The plots show the average number of individuals per patch for each species.

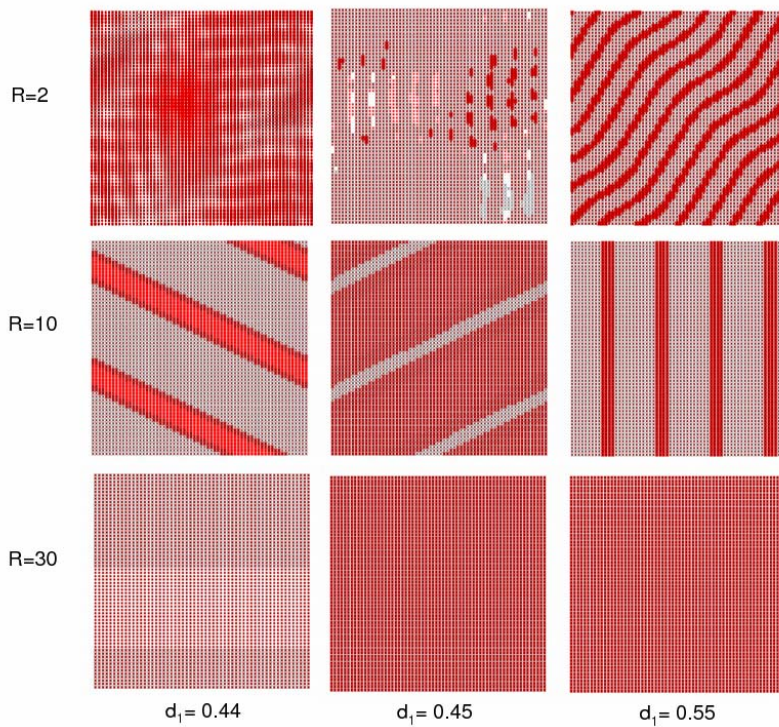


FIG. 6. (Color online) Spatial distribution after 10 000 time steps for periodic boundary conditions. The species x is plotted in black and y is in red (in black and white, dark regions correspond to higher concentrations of y).

the first 4000 as transient. If the two exponents turn out negative, the attractor is a periodic orbit or a fixed point; if one of them is negative and the other is zero, the attractor is a limit cycle; finally, if one of them is positive, the attractor is chaotic. Figure 4 shows three such attractors in the x - y space phase. Notice that, contrary to the continuous time model, the discrete dynamics of two species can display chaotic attractors. We found chaos only for the linear set of predation and feeding functions. Even so, for all values of d_1 with a positive Lyapunov exponent (see Fig. 3), the respec-

tive attractors take up only very small regions in phase space, similar to the situation illustrated in Fig. 4(a). Except for these small phase space areas displaying chaotic behavior the qualitative oscillatory variation of x and y is very similar to the HP model with $z=0$ and also to that obtained from the Lotka-Volterra equations [47].

B. Spatial model for two species

In this subsection we will show results only for the three values of d_1 shown in Fig. 4, corresponding to three different

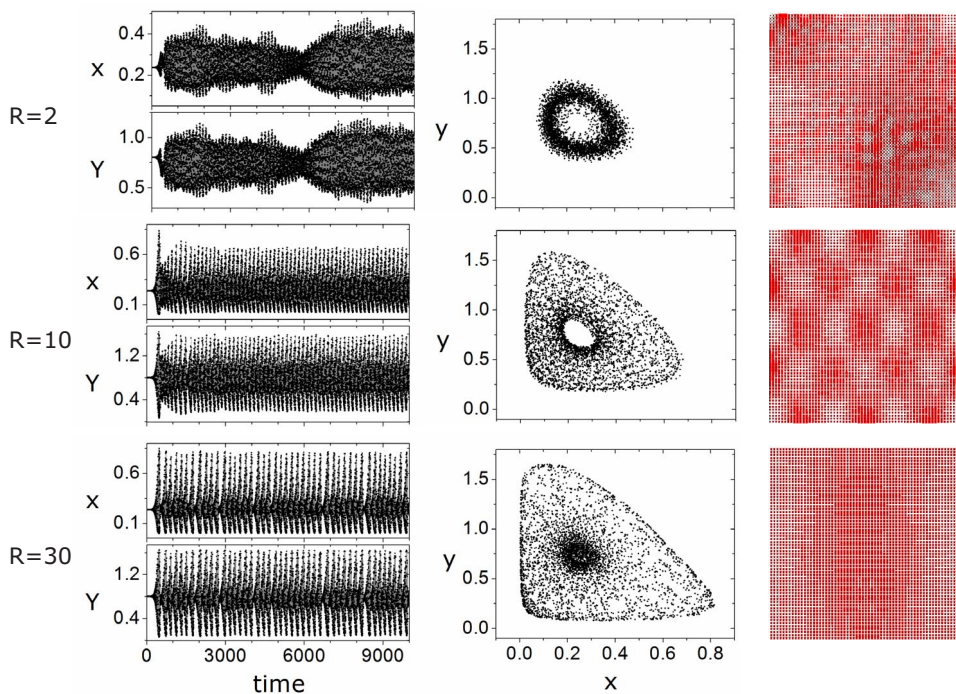


FIG. 7. (Color online) From the left to right: phase space attractors, temporal evolution of the average number of individuals, and patterns of spatial density, considering confined environment. The species x is plotted in black and y is in red (in black and white, dark regions correspond to higher concentrations of y).

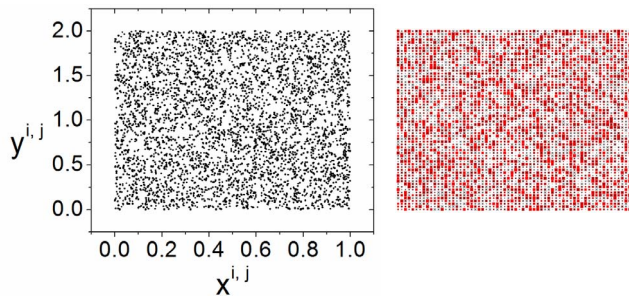


FIG. 8. (Color online) Phase space and the spatial population density at $t=0$. The species x is plotted in black and y is in red (in black and white, dark regions correspond to higher concentrations of y). Each point in the phase space plot corresponds to the initial condition of one patch.

kinds of attractors in the mean field model: chaotic ($d_1=0.44$), periodic orbit ($d_1=0.45$), and limit cycle ($d_1=0.55$). In all our simulations the initial conditions in each patch were chosen to be a fixed constant plus a random fluctuation with amplitude equal to 5% of this value. The value of the constant was chosen as that of the fixed point of the mean field model. We considered two types of boundary conditions: periodic (to simulate a large environment) and finite with hard walls (to simulate a confined environment or a nature reserve). Our main interest is to study the behavior of the populations as a function of the size of the predation radius.

1. Periodic boundary conditions

In order to compare the results of the spatial model with those of the mean field, we calculated the mean values of x and y over all sites by adding up the populations at each site and dividing by the total number of sites. Figure 5 shows phase space plots of the average populations for the three values of d_1 fixed above and three values of the predation radius R (we are dropping the subscript y in this section, since there is only one type of predator). The points shown are the last 4000 of a total of 10 000 time steps, except for the cases $R=10$ and $d_1=0.44$ and 0.45 . In these cases the transient lasts longer and we plotted the last 10 000 of 20 000 iterations.

For $R=2$ the predators prey upon 13 patches, approximately 0.3% of the lattice. The amplitude of the oscillations of the average values of x and y can be seen from Fig. 5 to be smaller than those in the mean field model. For the three values of d_1 considered the attractor becomes a fuzzy cycle. For $R=10$, there are 317 patches in the predation neighborhood, approximately 7.7% of the total. In this case, the amplitude of the oscillations increases and the attractors become thicker. For $d_1=0.44$ and $d_1=0.45$ the orbit takes about 7000 iterations to converge to the attractor. Finally, for $R=30$,

there are 2821 patches in the predation neighborhood, approximately 79% of the total. In this case, each predator can reach almost any patch, which is exactly the idea behind the mean field model. Indeed, the behavior shown in Fig. 5 for $R=30$ is very close to that predicted by the mean field model, Fig. 4.

Figure 6 displays the spatial patterns at $t=10\,000$ for the same parameters of Fig. 5. For $R=2$ density fluctuations are seen for all values of d_1 . As R increases these fluctuations become organized in stripes, that oscillate synchronously with the time. For $R=30$ the population distribution is nearly homogeneous, except for $d_1=0.44$, corresponding to the chaotic case in the mean field model, where the population density still displays two wide stripes.

2. Confined environment

To simulate a nature reserve or a small niche bounded by obstacles, the space was treated as a lattice with hard walls at the edges. Therefore predators located at a distance smaller than R from the boundary have a smaller predation neighborhood than individuals at the center of the lattice. Here we present results only for $d_1=0.44$, keeping the other parameters fixed as in the case of periodic boundary conditions.

Figure 7 shows the phase space attractors, the time evolution of the average populations, and the spatial patterns of population densities for $R=2$, $R=10$, and $R=30$. The main effect of the hard walls is to prevent the system from behaving like a totally mixing population, unless R is very close to the full size of the space available. Even for $R=30$, the presence of individuals close to the walls disrupt the system, producing different attractors in phase space and maintaining the spatial patterns.

3. Synchronization

The synchronization of coupled systems is a subject that has attracted a lot of attention in the past decade. In the

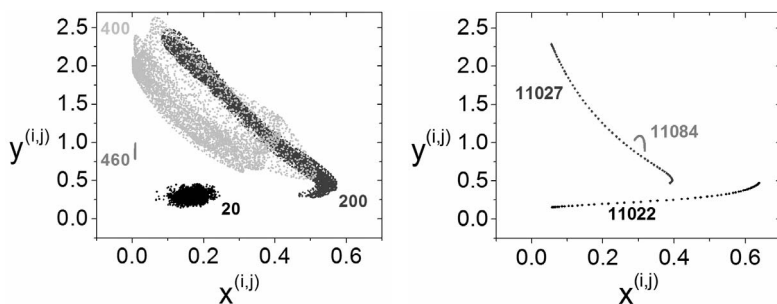


FIG. 9. Snapshots of the state of individual patches in phase space at different times. The left panel shows the transient period and the right panel shows the asymptotic regime.

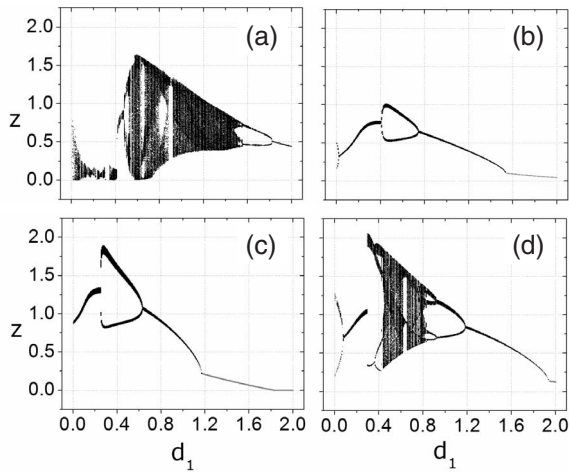


FIG. 10. Bifurcation diagrams for the four functional response sets: (a) I; (b) II; (c) III; (d) IV. The circles represent z_{max} (black) and the triangles (red) represent regimes where the dynamics converged to a fixed point.

present case, we can consider the populations at the patches as a set of mini ecosystems that interact through the predation neighborhoods and migration. The question of whether these systems can be synchronized even if they exhibit chaotic behavior is very interesting. The possibility of synchronized behavior is actually suggested by Fig. 6, where regions of the same color and intensity correspond to patches oscillating in phase. In order to see this in greater detail, we considered a situation where each patch has different (random) initial conditions and we followed the evolution of each of these patches in the phase space. Figure 8 shows the phase space and the spatial population density at time $t=0$. There are exactly $64 \times 64 = 4096$ points in this phase space diagram, representing the population of each patch in the spatial diagram, i.e., the state of all patches are plotted at initial time $t=0$. This is not to be confused with previously shown plots, where the average population of the whole set of patches were shown at several consecutive instants of time.

If the individuals in each patch were isolated and could not interact with others in different patches, i.e., $R=m_x=m_y$

$=0$, the trajectory corresponding to the evolution of the populations in each patch would follow exactly the same dynamics (corresponding, by construction, to that of the mean field model) and would end up in the same attractor, however, at different points within the attractor.

When individuals from different patches interact, the trajectories of the patches become correlated and tend to move together, like a swarm of bees. Figure 9 shows snapshots of the distribution of points in phase space at different times when $d_1=0.44$ and $R=10$. After a transient period, the populations evolve in a quasiperiodic fashion, alternating phases of highly synchronized motion ($t=11\,084$, for instance) with more spread out phases (like $t=11\,022$). This corresponds to uniform and striped spatial population densities, respectively (not shown).

V. THREE SPECIES

In this section we show numerical simulations for the case of three species. We shall see that not only is the dynamics richer in this case, presenting strange attractors and complex bifurcations diagrams, but that a new phenomenon appears, namely, outbreaks of predators. In order to reduce the number of parameters we fixed the migration rates at $m_x=0.01$, $m_y=0.1$, and $m_z=0.2$ and the death rate of the second predator at $d_2=0.65$.

A. Mean field model for three species

Similar to our procedure in the case of two species, we start by choosing one of the four functional response sets, Eqs. (7)–(9), or (10), before we proceed to a detailed analysis of the dynamics. Figure 10 shows the bifurcation diagrams for the functional response sets as a function of d_1 . This time the bifurcation diagram is defined as the maximum values attained by the variable z in each of its oscillations. Taking into account the richness of the diagrams, both the first and the fourth set would be interesting to study. We have chosen set IV because it corresponds to smooth feeding and predation functions and because its chaotic attractors resemble those of the HP model. This attractor is also very similar to that corresponding to the linear set I.

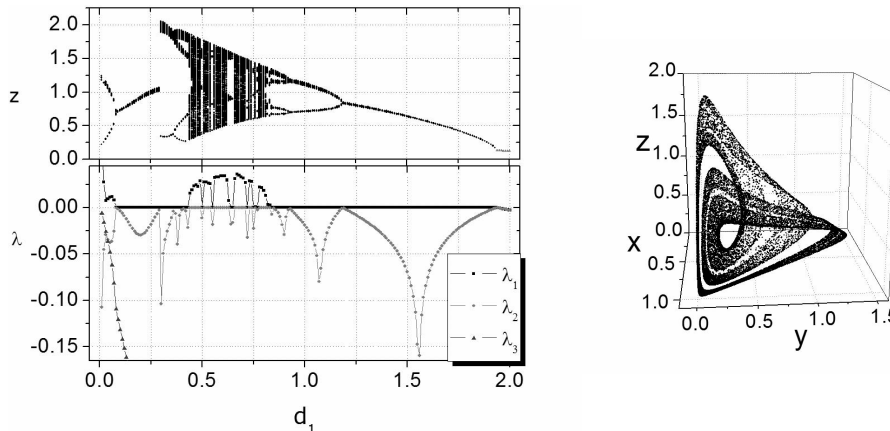


FIG. 11. Bifurcation diagram and Lyapunov exponents for the three species discrete time mean field model and response functions IV. The right panel shows the chaotic attractor for $d_1=0.44$.

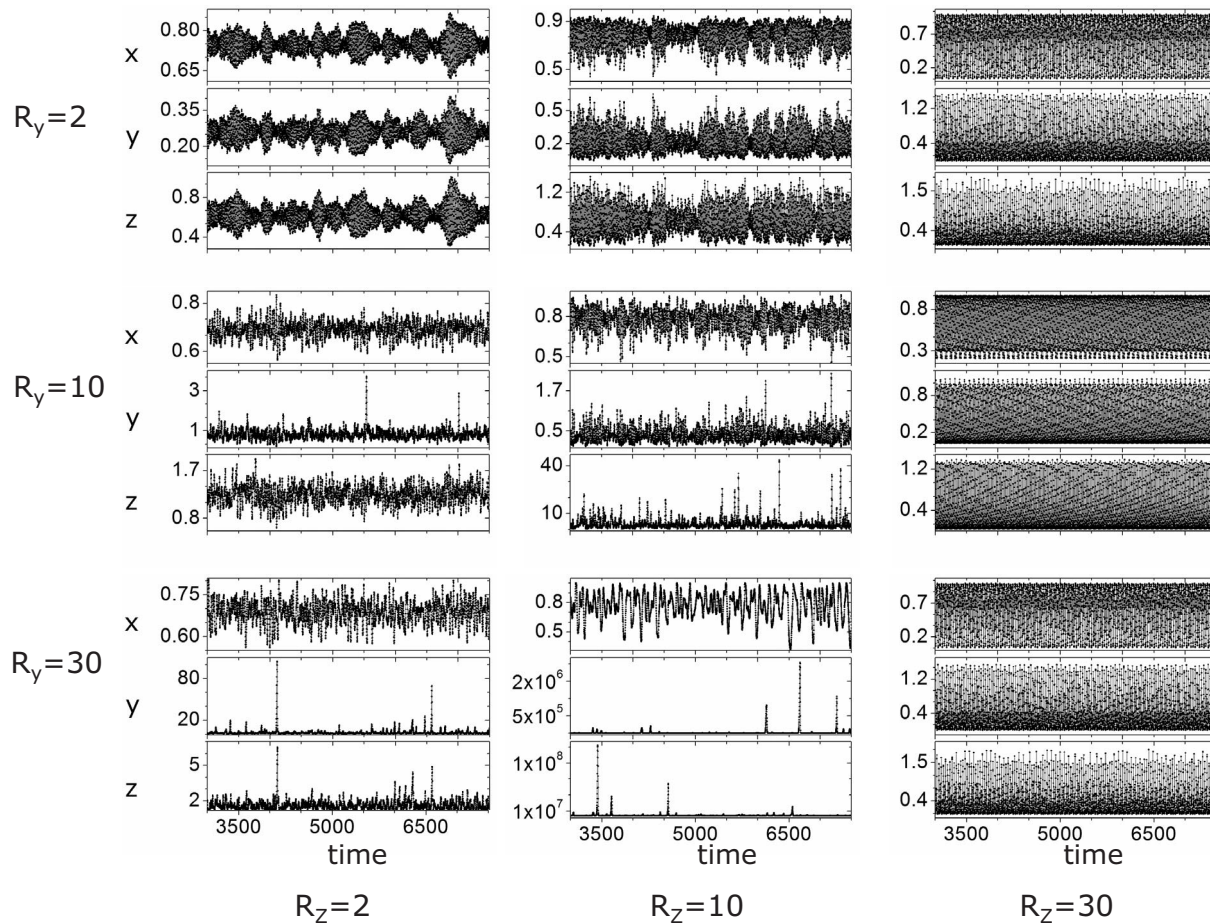


FIG. 12. Time evolution of the average number of individuals per patch between times 3 000 and 7 500, for periodic boundary conditions.

Figure 11 shows the bifurcation diagram and the Lyapunov exponents for the response functional set IV. A succession of bifurcations, similar to those found in the logistic map, can be observed as d_1 decreases. The right panel shows a typical chaotic attractor, for $d_1=0.44$.

B. Spatial model for three species

In this subsection we shall fix $d_1=0.44$ and focus our analysis on the role of the parameters R_y and R_z , the sizes of the predation neighborhoods for the y and z predators. Like in the case of two species, we also consider periodic or hard wall boundary conditions to simulate large or confined environments. In all our simulations the initial conditions for each patch were chosen as a fixed constant plus a random fluctuation with amplitude equal to 5% of this value. The value of the constant was chosen as that of the fixed point of the mean field model. The initial conditions were iterated for 10 000 time steps, unless stated otherwise.

1. Periodic boundary conditions

Figure 12 shows the time evolution in the interval from 3000 to 7500 iterations. Notice the different scales in each individual plot: for some values of R_y and R_z the populations of y and z increase significantly, displaying outbreaks of

short duration. Figure 13 shows the corresponding spatial patterns at the end of 10 000 iterations. The values attained by the y and z populations for $R_y=30$ and $R_z=10$ are strikingly high. A look at Eq. (14) reveals that, in fact, there is no restriction on the increase of y or z : they grow exponentially as long as $e^{-d} + F(\langle k_n \rangle_{R(i,j)}) > 1$. The outbreaks of predators, however, cannot last long, since they cause a rapid decrease in prey number. These *superpopulations* occur only when the predation radii assume intermediate values, not too small but not too large as compared to the size of the lattice. In all cases the populations return to the normal proportions observed in the mean field model as R_z approaches 30. When $R_y=R_z=30$ the spatial pattern is again homogeneous and the behavior is very similar to the mean field model.

Figure 14 shows the attractors in terms of the average number of individuals per patch for $R_z=30$ and different values of R_y . The attractors are well defined only for these values of the predation radii, where the spatial patterns are sufficiently simple. The presence of outbreaks leads to a diffuse distribution of points in the x - y - z space. For $R_z=30$ and R_y small, the interactions between the species are not strong enough to modify the dynamics in the individual patches. In this case the attractor is similar to the mean field model and the spatial density is homogeneous. When R_y assumes intermediate values, the spatial density displays checkerlike

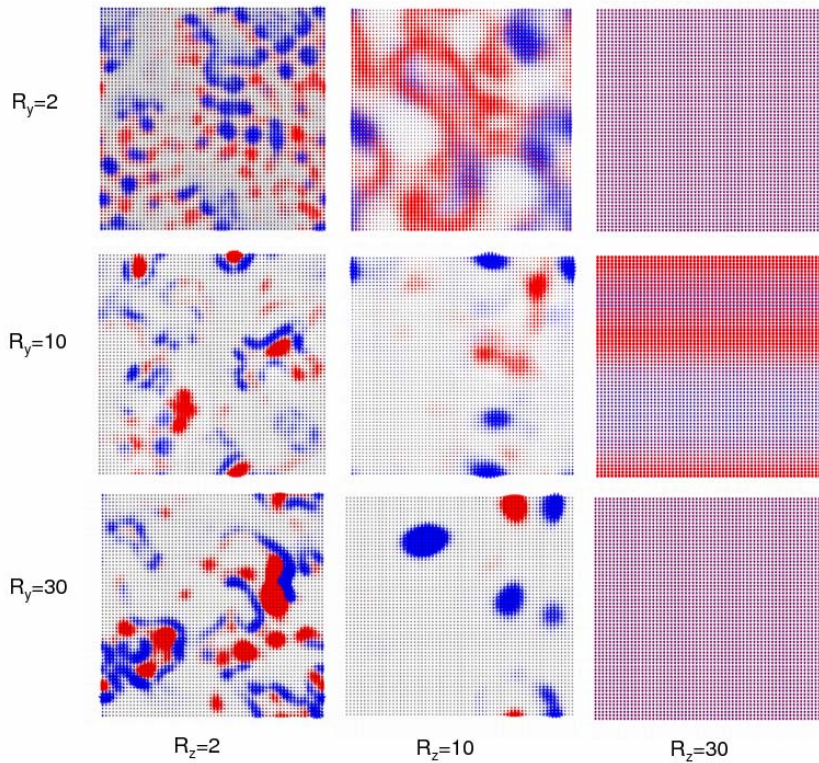


FIG. 13. (Color online) Spatial distribution after 10 000 iterations for periodic boundary conditions. Light gray represents x , displaying an approximately uniform distribution for all values of R_z and R_y ; red (gray) represents y and blue (dark gray) z . For $R_z=30$ and $R_y=10$ the darker region represents higher densities of both y and z .

structures and the attractor collapses to a nearly periodic motion with a few cycles. For $R_y=14$ the attractor reduces to a pure limit cycle and for $R_y=30$ the mean field attractor is fully restored.

2. Confined environments

When the environment is enclosed by hard walls, the predators that are near the borders have smaller predation neighborhoods than those near the center of the lattice. This results in an increase of the population of predators as compared to the case of periodic boundary conditions, giving rise to very large populations of predators. Figure 15 shows the spatial density at the end of 10 000 iterations. In general, the species x is homogeneously distributed in the space, while the predators y and z organize themselves in clusters. For small predation radii, the patterns are similar to those found in the case of periodic boundary conditions. The predators exhibit bursts of superpopulations concentrated in clusters that last for about 20 time steps and then fade away. The

bursts of y and z are out of phase, so that the absence of z makes y grow fast, which, in turn, triggers the subsequent growth of z . In general, the period of oscillation of the average populations is larger than the periods in each cluster. Figure 16 shows the time evolution of the average populations during 300 iterations when $R_y=30$ and $R_z=10$. In this situation the average values of y and z get as high as 10^6 . The clusters of species y usually occur close to the corners, which works as a protection against the z predators.

3. Synchronization

Once again, the spatial patterns displayed in Fig. 13 suggest that patches represented by the same color shades are synchronized. We studied the case $R_y=14$ and $R_z=30$ in more detail because its average attractor, shown in Fig. 14, is a simple limit cycle. We propagated random initial conditions for each patch and followed the dynamics for about 10 000 time steps. After a transient period the initial swarm of trajectories collapses into a finite set of points distributed

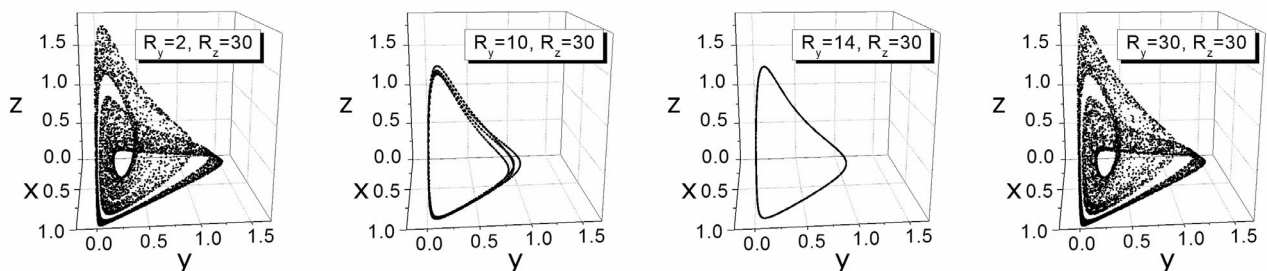


FIG. 14. Attractors for $R_z=30$ and different values of R_y .

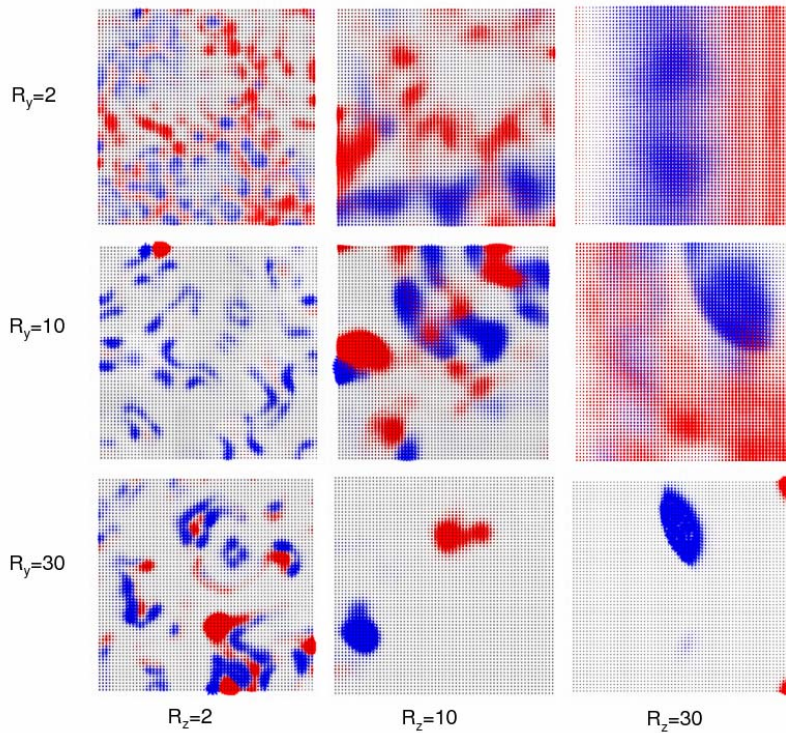


FIG. 15. (Color online) Spatial distribution after 10 000 iterations for the hard wall boundary conditions. Light gray represents x (displaying an approximately uniform distribution), red (gray) y and blue (dark gray) z .

along a line and the dynamics oscillates between homogeneous phases and phases with spatial striped patterns. Figure 17 shows snapshots of the distribution of points in phase space at different times after the transient period. The patterns refer to the same times as the snapshots. When the points in phase space are more scattered, $t=2504$ or $t=2509$, the spatial stripes are more visible. On the other hand, when the points in the phase space are closer, $t=2514$, the spatial distribution is nearly homogeneous.

To identify the orbit followed by each individual patch we studied the dynamics of eight patches, indexed by the coordinates (32, 8), (32, 16), (32, 24), (32,32), (32, 40), (32, 48), (32, 56), and (32, 64). These patches are located at the central vertical line of the square lattice, and their y coordinates are indicated in Fig. 17. From this figure it is clear that patches along horizontal lines are synchronized. Figure 18 displays the orbits of these eight selected patches, showing that different patches (actually different horizontal lines of patches) follow different attractors. The average orbit followed by the full set of patches is, surprisingly, a single limit cycle. Figure 18 shows that the eight selected patches follow only three different attractors and that some patches follow the same attractor in a different phase. All these attractors are limit cycles, one of them being a period-1 oscillation and the other two being period-2 oscillations.

Figure 19 shows that the attractors for the all the 4096 patches consist of a small set of closed curves. These attractors are strongly correlated and their average is the simple limit cycle presented in Fig. 14. This shows that the simple periodic behavior displayed by the average number of individuals actually hides a complex structure of oscillating patches that cannot be described by mean field models.

VI. DISCUSSION AND CONCLUSIONS

In this paper we constructed a spatial description of a food chain with two or three species based on the model of Hastings and Powell [35]. The key ingredients of the spatial model are the possibility of migration of individuals to nearby sites and the restriction imposed on predators to prey only in a certain neighborhood of their spatial location. We studied the transition between the regimes of local and long range interactions by changing the size of these predation neighborhoods from a few sites to the size of the whole available space.

In the case of two species we found that the discrete time mean field approach may introduce chaotic behavior, which is not found in the continuous time model. Chaos, however, appears only for linear predation and feeding functions and is restricted to small regions in phase space. When space is

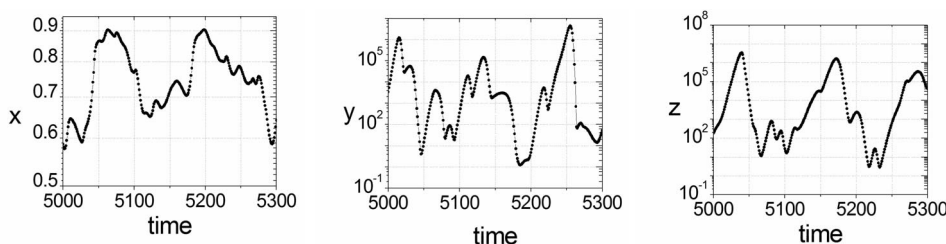


FIG. 16. Temporal evolution of the average number of individuals for the hard wall boundary conditions with $R_y=30$ and $R_z=10$.

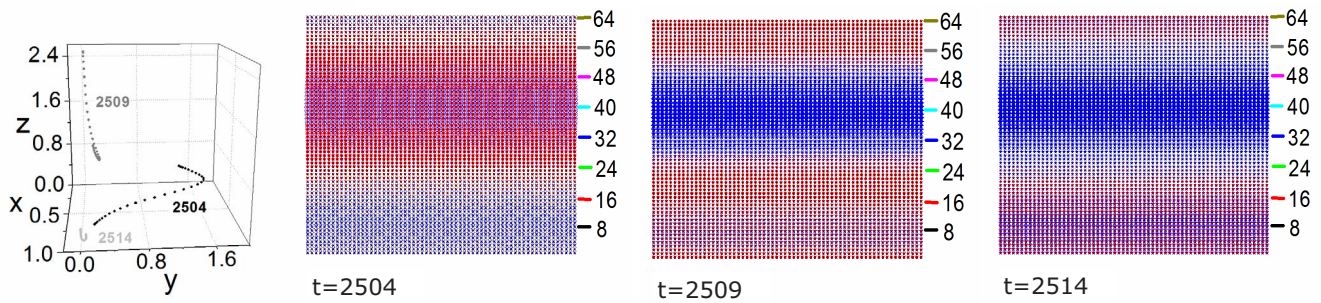


FIG. 17. (Color online) Phase space diagram for $R_y=14$ and $R_z=30$ at $t=2504$, $t=2509$, and $t=2514$, and spatial patterns for the same three times. For $t=2504$ the darker region represents higher densities of both y and z .

introduced, the population oscillations become more irregular, filling a ring in phase space instead of a simple curve. For the case of periodic boundary conditions the populations of predators and preys organize themselves in stripes that oscillate synchronically. As the size R of the predation neighborhood increases, the stripes become wider until they cover the whole space and the mean field limit with full synchrony is achieved. In phase space, however, the attractors first go from thin rings for small R to fat rings for intermediate values of R and then back to the simple mean field curves for large R (see Fig. 5). In the case of hard walls at the boundaries, the mean field limit is achieved only for larger values of the predation radius.

The introduction of a third species changes the dynamics of the system considerably. The behavior of the average populations as a function of the time becomes much more elaborate and the size of the two predation neighborhoods has dramatic effects on the population densities. We showed that the introduction of predation neighborhoods tend to suppress the appearance of chaos, reducing the attractors to simpler curves or even limit cycles. More importantly, our results show that when the size of the predation neighborhoods of the first predator R_y is large but that of the second predator R_z is small or intermediate, as compared to the size of the available space, outbreaks of predators arise for short periods of time. For confined environments the outbreaks are even more impressive, happening for a wider range of predation radii. The population of predators becomes highly concentrated in clusters whose subpopulations increase very fast and then almost disappear. These results suggest that the range of action of predators may be an important parameter in the dynamics of outbreaks. We speculate that the predation radius may be an important evolutionary trait, that would naturally evolve to an optimal value. To investigate this possibility, the model should be extended to describe an ecosystem in which the subpopulations on each patch were characterized by its own predation radius. However, more complicated behavior, such as periodic changes of the average predation radius, might occur [48].

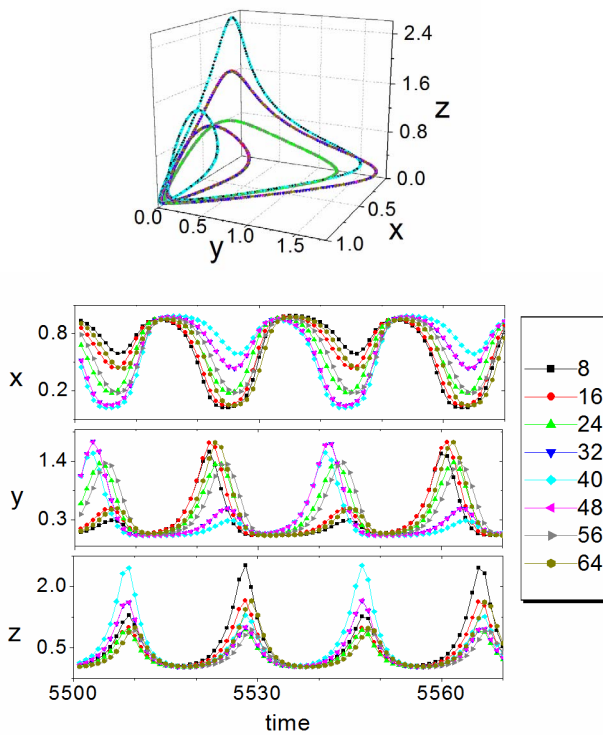


FIG. 18. (Color online) Three different attractors and their time evolution for eight different patches. The attractor reaching $z \approx 2.4$ corresponds to the curves labeled 8 and 40; the attractor reaching $z \approx 1.6$ to curves 16, 32, 48, and 64. The small, single loop attractor corresponds to curves 24 and 56.

Our study of synchronization showed that the periodic behavior of the average number of individuals in a spatially extended population may hide the existence of patches that oscillate out of phase in a highly coordinated fashion. The

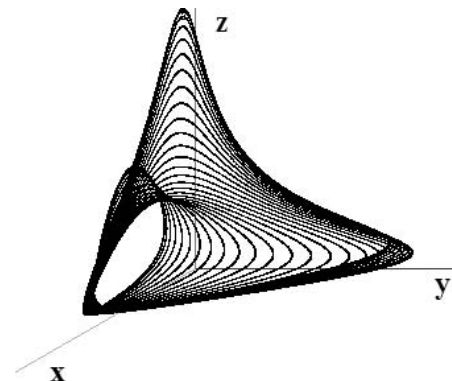


FIG. 19. Attractors for all the patches for $R_y=14$ and $R_z=30$.

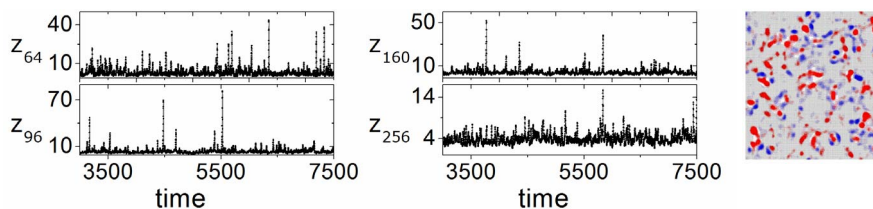


FIG. 20. (Color online) Time evolution of the average number of predators z for $R_y=R_z=10$ and different sizes of the lattice, $N=64$, $N=96$, $N=160$, and $N=256$ as indicated in the figure. The spatial pattern refers to the case where $N=256$ after 9000 iterations. Light gray represents x displaying an approximately uniform distribution, red (gray) is y , and blue (dark gray) is z .

limit cycle corresponding to the global average dynamics may be a composition of several different attractors governing the dynamics of synchronous patches.

All the simulations presented here were restricted to lattices with 64×64 sites. It is therefore important to discuss which of our results persist in larger lattices and which are eliminated in the so called thermodynamic limit, where the lattice size goes to infinity. We first recall that our model is designed in such a way that it always recovers the mean field approximation in the limit where the predation neighborhoods become of the order of the system size. On the other hand, features like the amplitude of the average population oscillations and the patterns of spatial density may change with the lattice size N . We illustrate the general behavior of the system with N with a few examples:

In the case of two species with $R=2$ and $d_1=0.55$ (see Figs. 5 and 6) the spatial striped pattern is maintained for $N=96$, although the attractor in phase space becomes thinner. When N is increased to 256 the attractor gets smaller and thicker, approaching a fixed point, but the spatial patterns get richer, mixing regions of stripes in different orientations and checkerlike structures in between. We believe that larger values of N would cause the attractor to collapse into a fixed point, in accordance with the results in Ref. [49]. The spatial

patterns, on the other hand, seem to persist even for very large lattices.

In the case of three species an important question is whether the outbreaks persist in very large lattices. We simulated the situation where $R_y=R_z=10$ (see Figs. 12 and 13) considering $N=96$, $N=160$, and $N=256$. Figure 20 shows the average value of z as a function of the time for the four lattices. The outbreaks do persist in these cases, but their amplitude seems to be either decreasing very slowly with N or even fluctuating. A detailed study of this behavior would require calculations with even larger lattices, with substantial computational requirements. The spatial pattern displayed for $N=256$ is very similar to that for $N=64$ and the populations in the clusters keep approximately the same proportion in both cases. This indicates that, even if the outbreaks of the average populations are washed out in the limit of infinite lattices, they may still persist locally in the individual clusters.

ACKNOWLEDGMENTS

This work was partially supported by Fapesp, CNPq, and Capes.

-
- [1] A. J. Lotka, *Elements of Physical Biology* (Williams and Wilkins, Baltimore, 1925).
 - [2] V. Volterra, *J. Cons., Cons. Int. Explor. Mer* **3**, 3 (1928).
 - [3] Richard Durrett and Simon Levin, *Theor Popul. Biol.* **46**, 363 (1994).
 - [4] *Spatial Ecology*, edited by David Tilman and Peter Kareiva, (Princeton University Press, Princeton, NJ, 1997).
 - [5] J. E. Satulovsky and T. Tome, *Phys. Rev. E* **49**, 5073 (1994).
 - [6] H. Sayama, L. Kaufman, and Y. Bar-Yam, *Phys. Rev. E* **62**, 7065 (2000).
 - [7] E. M. Rauch, H. Sayama, and Y. Bar-Yam, *J. Theor. Biol.* **221**, 655 (2003).
 - [8] M. A. Fuentes, M. N. Kuperman, and V. M. Kenkre, *Phys. Rev. Lett.* **91**, 158104 (2003).
 - [9] M. A. M. de Aguiar, E. M. Rauch, and Y. Bar-Yam, *Phys. Rev. E* **67**, 047102 (2003).
 - [10] M. A. M. de Aguiar, H. Sayama, M. Baranger, and Y. Bar-Yam, *J. Stat. Phys.* **114**, 1417 (2004).
 - [11] M. Mobilia, I. T. Georgiev, and U. C. Tauber, *Phys. Rev. E* **73**, 040903(R) (2006).
 - [12] T. Reichenbach, M. Mobilia, and E. Frey, *Phys. Rev. E* **74**, 051907 (2006).
 - [13] S. Strogatz, *Sync: The Emerging Science of Spontaneous Order* (Hyperion, New York, 2003).
 - [14] N. M. Ferguson, R. M. May, and R. M. Anderson, in *Spatial Ecology*, edited by David Tilman and Peter Kareiva (Princeton University Press, Princeton, NJ, 1997).
 - [15] O. Huito, J. Laaksonem, K. Norrdahl, and E. Korpimäki, *Oikos* **109**, 583 (2005).
 - [16] E. Ranta, V. Kaitala, and P. Lundberg, *Science* **278**, 1621 (1997).
 - [17] B. Blasius, A. Huppert, and L. Stone, *Nature (London)* **399**, 354 (1999).
 - [18] L. Becks, F. M. Hilker, H. Malchow, K. Jurgens, and H. Arndt, *Nature (London)* **435**, 1226 (2005).
 - [19] C. J. Daniel and J. H. Myers, *Ecography* **18**, 353 (1995).
 - [20] J. H. Myers, *Ecology* **79**, 1111 (1998).
 - [21] D. W. Williams and A. M. Liebhold, *Ecology* **81**, 2753 (2000).

- [22] M. Peltonen, A. M. Liebhold, O. N. Bjornstad, and D. W. Williams, *Ecology* **83**, 3120 (2002).
- [23] B. H. Aukema, A. L. Carroll, J. Zhu, K. F. Raffa, T. A. Sickley, and S. W. Taylor, *Ecography* **29**, 427 (2006).
- [24] B. J. Cooke and F. Lorenzetti, *Forest Ecol. Manage.* **226**, 110 (2006).
- [25] L. M. Pecora and T. L. Carroll, *Phys. Rev. Lett.* **64**, 821 (1990).
- [26] L. M. Pecora, T. L. Carroll, G. A. Johnson, and D. J. Mar, *Chaos* **7**, 520 (1997).
- [27] D. H. Zanette and A. S. Mikhailov, *Phys. Rev. E* **58**, 872 (1998).
- [28] F. S. de San Roman, S. Boccaletti, D. Maza, and H. Mancini, *Phys. Rev. Lett.* **81**, 3639 (1998); **82**, 674 (1999).
- [29] R. L. Viana and C. Grebogi, *Phys. Rev. E* **62**, 462 (2000).
- [30] C. M. Kim, S. Rim, and W. H. Kye, *Phys. Rev. Lett.* **88**, 014103 (2002).
- [31] S. Boccaletti, J. Kurths, G. Osipov, D. L. Valladares, and C. S. Zhou, *Phys. Rep.* **366**, 1 (2002).
- [32] H. L. D. S. Cavalcante and J. R. Rios Leite, *Chaos* **13**, 209 (2003).
- [33] S. Jalan and R. E. Amritkar, *Phys. Rev. Lett.* **90**, 014101 (2003).
- [34] K. E. Lonngren, E. W. Bai, and A. Ucar, *Chaos, Solitons Fractals* **20**, 387 (2004).
- [35] A. Hastings and T. Powell, *Ecology* **72**, 896 (1991).
- [36] C. S. Holling, *Can. Entomol.* **91**, 385 (1959).
- [37] S. Ellner and P. Turchin, *Am. Nat.* **145**, 343 (1995).
- [38] G. F. Fussmann and G. Heber, *Ecol. Lett.* **5**, 394 (2002).
- [39] J. Chattopadhyay and R. R. Sarkar, *Ecol. Modell.* **163**, 45 (2003).
- [40] D. O. Maionchi, S. F. dos Reis, and M. A. M. de Aguiar, *Ecol. Modell.* **191**, 291 (2006).
- [41] Andrew P. Beckerman, *Oikos* **110**, 591 (2005).
- [42] Hiroki Sayama, M. A. M. de Aguiar, Yaneer Bar-Yam, and Michel Baranger, *Phys. Rev. E* **65**, 051919 (2002).
- [43] M. A. M. de Aguiar, Michel Baranger, Yaneer Bar-Yam, and Hiroki Sayama, *Braz. J. Phys.* **33**, 514 (2003).
- [44] Ilkka A. Hanski and Michael E. Gilpin, *Metapopulation Biology: Ecology, Genetics, and Evolution* (Academic Press, New York, 1997).
- [45] *The Geometry of Ecological Interactions*, edited by U. Dieckmann, R. Law, and A. J. Metz (Cambridge University Press, Cambridge, England, 2000).
- [46] T. M. Janaki, Govindan Rangarajan, Salman Habib, and Robert D. Ryne, *Phys. Rev. E* **60**, 6614 (1999).
- [47] Ricard V. Solé and Jordi Bascompte, *Self-Organization in Complex Systems*, Monographs in Population Biology (Princeton University Press, Princeton, NJ, 2006).
- [48] A. Lipowski, *Phys. Rev. E* **71**, 052902 (2005).
- [49] M. Kowalik, A. Lipowski, and A. L. Ferreira, *Phys. Rev. E* **66**, 066107 (2002).